DESY 96–131
WUE–ITP–96–016
August 1996

The Evolution of Unpolarized and Polarized Structure Functions at Small x*

J. Blümlein, S. Riemersma

DESY–Zeuthen
Platanenallee 6, D–15735 Zeuthen, Germany

A. Vogt

Institut für Theoretische Physik, Universität Würzburg
Am Hubland, D–97074 Würzburg, Germany

Abstract

A survey is given of recent developments on the resummed small-x evolution, in a framework based on the renormalization group equation, of non–singlet and singlet structure functions in both unpolarized and polarized deep–inelastic scattering. The available resummed anomalous dimensions are discussed for all these cases, and the most important analytic and numerical results are compiled. The quantitative effects of these small-x resummations on the evolution of the various parton densities and structure functions are presented, and their present uncertainties are investigated. An application to QED radiative corrections is given.

* Based on invited talks presented by J. Blümlein at the International Workshop on Deep Inelastic Scattering and Related Phenomena (DIS'96), Rome, Italy, April 1996; and by A. Vogt at the 1996 Zeuthen Workshop on Elementary Particle Theory: QCD and QED in Higher Orders, Rheinsberg, Germany, April 1996. To appear in the Proceedings of the Rheinsberg Workshop, Nucl. Phys. **B** (Proc. Suppl.).

The Evolution of Unpolarized and Polarized Structure Functions at Small x*

J. Blümlein [a], S. Riemersma [a], and A. Vogt [b]

[a]DESY–Zeuthen, Platanenallee 6, D–15735 Zeuthen, Germany

[b]Institut für Theoretische Physik, Universität Würzburg, Am Hubland, D–97074 Würzburg, Germany

A survey is given of recent developments on the resummed small-x evolution, in a framework based on the renormalization group equation, of non–singlet and singlet structure functions in both unpolarized and polarized deep–inelastic scattering. The available resummed anomalous dimensions are discussed for all these cases, and the most important analytic and numerical results are compiled. The quantitative effects of these small-x resummations on the evolution of the various parton densities and structure functions are presented, and their present uncertainties are investigated. An application to QED radiative corrections is given.

1. Introduction

The evolution kernels of both non–singlet and singlet, unpolarized and polarized parton densities contain large logarithmic contributions for small fractional momenta x. For unpolarized deep–inelastic scattering (DIS) processes the leading small-x contributions in the singlet case behave like [1]

$$\left(\frac{\alpha_s}{N-1}\right)^k \quad \leftrightarrow \quad \frac{1}{x}\,\alpha_s^k\,\ln^{k-1} x \;\;,$$

where N is the Mellin variable. The leading terms for the unpolarized and polarized non–singlet and the polarized singlet cases are of the form [2,3]

$$N\left(\frac{\alpha_s}{N^2}\right)^k \quad \leftrightarrow \quad \alpha_s^k\,\ln^{2k-2} x \;\;.$$

The resummation of these terms to all orders in the strong coupling constant α_s can be completely derived by means of perturbative QCD. Since infinities, such as the ultraviolet and collinear divergencies, emerging in the calculation of the higher–order corrections have to be dealt with, the *only* appropriate framework for carrying out these resummations is provided by the renormalization group equations. The impact of the resulting all–order anomalous dimensions on the behaviour of the DIS structure functions at small x depends as well on the non–perturbative input parton densities at an initial scale Q_0^2. Thus the resummation effects can only be studied via the evolution over some range in Q^2.

This evolution moreover probes the anomalous dimensions also at medium and large values of x by the Mellin convolution with the parton densities. Hence the small-x dominance of the leading terms over contributions less singular as $x \to 0$ in the anomalous dimensions does *not* necessarily imply the same situation for observable quantities, such as the structure functions. These aspects need to be considered to arrive at sound conclusions about the consequences of the small-x resummations on physical quantities.

In the present paper we give a survey of the recent developments in this field. The general framework for the evolution of parton densities and structure functions is recalled in Section 2. Section 3 reviews the available results on the resummed anomalous dimensions for the various DIS processes. Numerical coefficients for their expansions in α_s are compiled, as well as the analytical predictions for the most singular contributions to the 3–loop splitting functions. The issue of subleading terms is discussed, guided by the known 2–loop results. In Section 4 the numerical implication of these resummations are investigated for the various unpolarized and polarized cases. The uncertainties due to possible less singular terms and due to insufficiently constrained initial parton densities are illustrated. An application to QED radiative corrections is presented. Section 5 summarizes the main results.

*Talk presented by A. Vogt

2. The evolution equations

The twist-2 contributions to any deep–inelastic scattering structure function can be represented in general, see e.g. [4,5], by the three flavour non–singlet combinations of quark densities

$$q^{\pm}_{\rm NS,i} = q_i \pm \overline{q}_i - \frac{1}{N_f}\sum_{r=1}^{N_f}(q_r \pm \overline{q}_r)\,, \quad (1)$$

$$q^{\rm val}_{\rm NS} = \sum_{r=1}^{N_f}(q_r - \overline{q}_r)\,, \quad (2)$$

and the singlet quark and gluon distributions

$$\boldsymbol{q}_S = \begin{pmatrix} \Sigma \\ g \end{pmatrix}\,,\ \Sigma \equiv \sum_{r=1}^{N_f}(q_r + \bar{q}_r)\,. \quad (3)$$

Here N_f denotes the number of active (massless) quark flavours. The structure functions $F_i(x,Q^2)$ are obtained by

$$F_i(x,Q^2) = \sum_{r=1}^{2N_f} a_{ir}\, c_{i,r}(x,Q^2)\otimes q_r(x,Q^2) + a_{ig}\, c_{i,g}(x,Q^2)\otimes g(x,Q^2)\,, \quad (4)$$

where the factors a_{ij} depend on the electroweak couplings, and $c_{i,j}(x,Q^2)$ denote the respective coefficient functions. Finally $\otimes$ stands for the Mellin convolution in the first variable,

$$A(x)\otimes B(x) = \int_0^1 dx_1 \int_0^1 dx_2\, \delta(x - x_1x_2)\, A(x_1)B(x_2)\,. \quad (5)$$

The above notation is used in a generic way for both unpolarized and polarized DIS, i.e. for the polarized case the replacements

$$q \to \Delta q\,,\quad \overline{q} \to \Delta\overline{q}\,,\quad \text{and}\ \ g \to \Delta g, \quad (6)$$

are understood with, e.g., Δq given in terms of the spin projections $q\uparrow$ and $q\downarrow$ via

$$\Delta q = q\uparrow - q\downarrow\ . \quad (7)$$

Correspondingly the splitting functions (see below) and the coefficient functions in eq. (4) have to be replaced.

As long as the splitting functions P^S_{qq} and $P^S_{q\overline{q}}$ (cf. ref. [4]) do not differ, the evolution equations are identical for the combinations $q^-_{{\rm NS},i}$ and $q^{\rm val}_{\rm NS}$. Since this is the case at all orders known presently (i.e. up to next-to-leading order, NLO)[2], we will not investigate the evolution of the combination (2) separately in the following.

The evolution equations for the non–singlet and singlet combinations of the parton distributions are then given by

$$\frac{\partial\, q^{\pm}_{\rm NS}(x,Q^2)}{\partial \ln Q^2} = P^{\pm}_{\rm NS}(x,\alpha_s)\otimes q^{\pm}_{\rm NS}(x,Q^2)\,,$$
$$\frac{\partial\, \boldsymbol{q}_{\rm S}(x,Q^2)}{\partial \ln Q^2} = \boldsymbol{P}_{\rm S}(x,\alpha_s)\otimes \boldsymbol{q}_{\rm S}(x,Q^2)\,. \quad (8)$$

The splitting functions $P^{\pm}_{\rm NS}$ and $\boldsymbol{P}_{\rm S}$ are specified below. Note that the unpolarized (polarized) quark density combinations $q^-_{\rm NS}$ and $q^+_{\rm NS}$ evolve with $P^-_{\rm NS}$ ($P^+_{\rm NS}$) and $P^+_{\rm NS}$ ($P^-_{\rm NS}$), respectively.

In the following, we will simplify the notation by dropping the subscripts 'NS' and 'S', and use the abbreviation $a_s \equiv \alpha_s(Q^2)/4\pi$ for the running QCD coupling for convenience. The scale dependence of a_s is governed by

$$\frac{da_s}{d\ln Q^2} = -\sum_{k=0}^{\infty} a_s^{k+2}\beta_k\,, \quad (9)$$

where only $\beta_0 = (11/3)\,C_A - (4/3)\,T_F N_f$ and $\beta_1 = (34/3)\,C_A^2 - (20/3)\,C_A T_F N_f - 4\,C_F T_F N_f$ enter up to NLO. The colour factors are $C_F = (N_c^2-1)/(2N_c) \equiv 4/3$, $C_A = N_c \equiv 3$, $T_F = 1/2$. For the numerical calculations in Section 4 we use

$$a_s = \frac{1}{\beta_0}\ln(Q^2/\Lambda^2)\left[1 - \frac{\beta_1 \ln\ln(Q^2/\Lambda^2)}{\beta_0^2\ln(Q^2/\Lambda^2)}\right], \quad (10)$$

with Λ being the QCD scale parameter. The splitting functions and coefficient functions can be represented by the series

$$P^{\pm}(x,a_s) = \sum_{l=0}^{\infty} a_s^{l+1} P^{\pm}_l(x)\,,$$
$$\boldsymbol{P}(x,a_s) \equiv \begin{pmatrix} P_{qq}(x,a_s) & P_{qg}(x,a_s) \\ P_{gq}(x,a_s) & P_{gg}(x,a_s)\end{pmatrix} = \sum_{l=0}^{\infty} a_s^{l+1}\boldsymbol{P}_l(x)\,, \quad (11)$$

[2] So far only for the anomalous dimension $\gamma^+_{\rm NS}$ the first moments have been calculated to 3–loop order [6].

$$c_{i,j}(x,Q^2) \;=\; \delta(1-x)\delta_{jq} + \sum_{l=1}^{\infty} a_s^l c_{ij,l}(x)\,. \quad (12)$$

Unless another scheme is stated explicitly, we will always refer to the $\overline{\rm MS}$ scheme both for renormalization and factorization, and take Q^2 as the renormalization and factorization scale.

The expansion coefficients $P_l^-(x)$ and $\boldsymbol{P}_l^{\rm unpol}(x)$ are subject to the sum rules

$$\int_0^1 dx\, P_l^-(x) = 0\,,$$
$$\int_0^1 dx\, x \sum_i P_{ij,l}^{\rm unpol.}(x) = 0\,, \quad (13)$$

which are due to fermion number and energy momentum conservation, respectively. By now all the unpolarized and polarized splitting functions are completely known up to NLO, $l = 1$. The full expressions for their x–dependences can be found in refs. [7]–[11]. The most singular contributions as $x \to 0$ will be displayed in Section 3.4.

The parton densities are not observables beyond leading order. Hence it is convenient to consider also the evolution equations for related physical quantities, the structure functions $F_i(x,Q^2)$, directly. In non–singlet cases, the all–order resummation of the leading small-x contributions has in fact been given [2] on the level of the structure function combinations $F_i^{\pm}(x,Q^2)$. Their evolution equations read

$$\frac{\partial\, F_i^{\pm}(x,a_s)}{\partial a_s} = -\frac{1}{\beta_0 a_s^2} K_i^{\pm}(x,a_s) \otimes F_i^{\pm}(x,a_s) \quad (14)$$

after a transformation to an equation in a_s. Here, e.g., the NLO kernels can be written as

$$K_{i,1}^{\pm}(x,a_s) = \quad (15)$$
$$a_s\, P_0(x) + a_s^2 \left[P_1^{\pm}(x) - \frac{\beta_1}{\beta_0} P_0(x) - \beta_0 c_{i,1}^{\pm}(x) \right],$$

with $c_i^{\pm}(x)$ denoting the corresponding coefficient function combinations. Generally the terms $\propto a_s (a_s \ln^2 x)^l$ emerge in the a_s expansion of the kernels $K_i^{\pm}(x,a_s)$ only in combination with the coefficient β_0. As will be outlined below the leading small-x contributions to these kernels coincide with those of the $\overline{\rm MS}$ splitting functions $P_l^{\pm}(x)$, since the corresponding coefficient functions $c_{i,l}^{\pm}(x)$ turn out to be less singular as $x \to 0$.

3. Resummation of leading small-x terms

3.1. The non-singlet case

The most singular contributions to the Mellin transforms of the all–order evolution kernels $K^{\pm}(x,a_s)$ for the non–singlet structure functions have been obtained via

$$\mathcal{M}\left[K_{x\to 0}^{\pm}(a_s)\right](N) \equiv \int_0^1 dx\, x^{N-1} K_{x\to 0}^{\pm}(x,a_s)$$
$$\equiv -\frac{1}{2}\,\boldsymbol{\Gamma}_{x\to 0}^{\pm}(N,a_s) = \frac{1}{8\pi^2} f_0^{\pm}(N,a_s) \quad (16)$$

from positive and negative signature amplitudes $f_0^{\pm}(N,a_s)$ studied in ref. [2] (cf. Section 3.2):

$$\boldsymbol{\Gamma}_{x\to 0}^{+}(N,a_s) = -N\left\{1 - \sqrt{1 - \frac{8a_sC_F}{N^2}}\right\},$$
$$\boldsymbol{\Gamma}_{x\to 0}^{-}(N,a_s) = \quad (17)$$
$$-N\left\{1 - \sqrt{1 - \frac{8a_sC_F}{N^2}\left[1 - \frac{f_8^+(N,a_s)}{2\pi^2 N}\right]}\right\}.$$

Here the colour octet amplitude $f_8^+(N,a_s)$ reads

$$f_8^+(N,a_s) = 16\pi^2 N_c a_s \frac{d}{dN} \ln\left[e^{\,z^2/4} D_{-1/[2N_c^2]}(z)\right] \quad (18)$$

with $z = N/\sqrt{2N_c a_s}$ and $D_p(z)$ denoting the parabolic cylinder function [12].

Expanding the resummed anomalous dimensions (17) into a series in a_s and transforming

l	K_l^+	K_l^-
0	2.667E0	2.667E0
1	3.556E0	5.333E0
2	1.580E0	1.432E0
3	3.512E-1	9.964E-1
4	4.682E-2	-2.078E-1
5	4.162E-3	1.448E-1
6	2.643E-4	-5.777E-2
7	1.258E-5	2.168E-2
8	4.661E-7	-7.173E-3
9	1.381E-8	2.143E-3
10	3.348E-10	-5.827E-4

Table 1: The coefficients $K_l^{\pm}$ of the expansion of $K_{x\to 0}^{\pm}(x,a_s)$ in terms of $a_s(a_s \ln^2 x)^l$ as obtained from the resummations in eqs. (17) and (18).

back to x–space yields the numerical coefficients shown in Table 1. The first two terms of the resummed kernel $K^{\pm}_{x\to 0}(x,a_s)$ agree with the leading small-x contributions of the corresponding LO and NLO splitting functions $P^{\pm}(x,a_s)$ [13]. This expansion also reveals a significant theoretical difference between $\mathbf{\Gamma}^{+}_{x\to 0}(N,a_s)$ and $\mathbf{\Gamma}^{-}_{x\to 0}(N,a_s)$: the a_s series is convergent in the former but not in the latter case, where it involves the asymptotic expansion of $D_p(z)$.

Unlike the splitting functions, the coefficient functions $c^{\pm}_i(x,a_s)$ are known up to next-to-next-to-leading order (NNLO), $l = 2$, in the $\overline{\rm MS}$ scheme [14,15]. At small x they rise only as

$$c^{\pm}_{i,1} \propto \ln x\,, \quad c^{\pm}_{i,2} \propto \ln^3 x\,. \tag{19}$$

Therefore the third expansion coefficient of $K^{\pm}_{x\to 0}(x,a_s)$ leads to a prediction for the most singular parts of the non–singlet $\overline{\rm MS}$ splitting functions in NNLO, $P^{\pm}_2(x)$, given by [13]

$$P^{+}_{2,\,x\to 0}(x) = \frac{2}{3}C_F^3 \ln^4 x\,, \tag{20}$$

$$P^{-}_{2,\,x\to 0}(x) = \left[-\frac{10}{3}C_F^3 + 4C_F^2C_A - C_FC_A^2\right]\ln^4 x\,.$$

All the methods of this section have been applied to QED and also comparisons with the available fixed order calculations were carried out. For details we refer to refs. [16,17].

3.2. The polarized singlet case

The amplitude relations of ref. [2] have been generalized to the polarized singlet case recently [3]:

$$\boldsymbol{F}_0(N,a_s) = 16\pi^2\frac{a_s}{N}\boldsymbol{M}_0 \tag{21}$$
$$-\frac{8a_s}{N^2}\boldsymbol{F}_8(N,a_s)\boldsymbol{G}_0 + \frac{1}{8\pi^2}\frac{1}{N}\boldsymbol{F}_0^2(N,a_s)\,,$$
$$\boldsymbol{F}_8(N,a_s) = 16\pi^2\frac{a_s}{N}\boldsymbol{M}_8 \tag{22}$$
$$+\frac{2a_s}{N}C_G\frac{d}{dN}\boldsymbol{F}_8(N,a_s) + \frac{1}{8\pi^2}\frac{1}{N}\boldsymbol{F}_8^2(N,a_s)\,.$$

Here the basic matrices are given by

$$\boldsymbol{M}_0 = \begin{pmatrix} C_F & -2T_FN_f \\ 2C_F & 4C_A \end{pmatrix},\ \boldsymbol{G}_0 = \begin{pmatrix} C_F & 0 \\ 0 & C_A \end{pmatrix},$$
$$\boldsymbol{M}_8 = \begin{pmatrix} C_F - C_A/2 & -T_FN_f \\ C_A & 2C_A \end{pmatrix}. \tag{23}$$

Note that the matrix $\boldsymbol{M}_0$ is the $x \to 0$ limit of the well–known matrix of the polarized splitting functions in LO [8]. The equations for $f^{\pm}_0(N,a_s)$ and $f^{+}_8(N,a_s)$ of Section 3.1 are entailed in these expressions by keeping only the qq-entries of the matrices (23), and, in the '+'-case, additionally dropping the $\boldsymbol{F}_8$-term in eq. (21). Also for the polarized singlet structure function $g_1(x,Q^2)$ the coefficient functions are known up to NNLO [15], and their leading small-x behaviour is the same as in eq. (19). The resummed leading small-x contributions to the splitting functions are thus related to $\boldsymbol{F}_0(N,a_s)$ by

$$\begin{aligned}\boldsymbol{P}(x,a_s)_{x\to 0} &= \sum_{l=0}^{\infty}\boldsymbol{P}_l^{x\to 0}(x)\,a_s^{l+1} \\ &= \frac{1}{8\pi^2}\mathcal{M}^{-1}\left[\boldsymbol{F}_0(N,a_s)\right](x)\,.\end{aligned} \tag{24}$$

Eqs. (21) and (23) have been solved directly in terms of a series in a_s in ref. [18]. Unlike the previous non–singlet case, the representation (24) is needed for the analytical N-space solution of the evolution equations here, cf. Section 4.3. Also in the present case the lowest–order expansion coefficients $\boldsymbol{P}_{0,1}^{x\to 0}(x)$ agree with the corresponding limit of the NLO splitting function matrices [3]. The predictions for the NNLO quantities $P_{ij,2}^{x\to 0}$ read [18]:

$$\begin{aligned}P_{qq,2}^{x\to 0}(x) &= \frac{2}{3}C_F\Big[-5\,C_F^2 - \frac{3}{2}\,C_A^2 + 6\,C_A\,C_F \\ &\quad - 8\,T_FN_f\,C_F - 6\,T_FN_f\,C_A\Big]\ln^4 x\,, \\ P_{qg,2}^{x\to 0}(x) &= \frac{2}{3}T_FN_f\Big[-15\,C_A^2 + 2\,C_F^2 - 6\,C_F\,C_A \\ &\quad + 8\,T_FN_fC_F\Big]\ln^4 x\,, \\ P_{gq,2}^{x\to 0}(x) &= \frac{2}{3}C_F\Big[15\,C_A^2 - 2\,C_F^2 + 6\,C_F\,C_A \\ &\quad - 8\,T_FN_fC_F\Big]\ln^4 x\,, \\ P_{gg,2}^{x\to 0}(x) &= \frac{2}{3}\Big[28\,C_A^3 + 2\,T_FN_f\,C_A^2 - 4T_FN_f\,C_F^2 \\ &\quad - 24\,C_F\,T_FN_f\,C_A\Big]\ln^4 x\,.\end{aligned} \tag{25}$$

The expansion coefficients up to $l = 10$ are shown in a compact numerical form in Table 2. For a more precise representation see ref. [18].

	$N_f = 3$			
l	$P_{qq}^{(l)}$	$P_{qg}^{(l)}$	$P_{gq}^{(l)}$	$P_{gg}^{(l)}$
0	2.667E0	-6.000E0	5.333E0	2.400E1
1	-1.067E1	-4.400E1	3.911E1	1.280E2
2	-3.679E1	-1.394E2	1.240E2	4.189E2
3	-6.642E1	-2.288E2	2.034E2	6.981E2
4	-6.110E1	-2.154E2	1.915E2	6.685E2
5	-3.858E1	-1.347E2	1.197E2	4.201E2
6	-1.680E1	-5.955E1	5.294E1	1.868E2
7	-5.632E0	-1.979E1	1.759E1	6.213E1
8	-1.424E0	-5.082E0	4.517E0	1.602E1
9	-2.991E-1	-1.050E0	9.331E-1	3.303E0
10	-4.869E-1	-1.757E-1	1.562E-1	5.557E-1
	$N_f = 4$			
l	$P_{qq}^{(l)}$	$P_{qg}^{(l)}$	$P_{gq}^{(l)}$	$P_{gg}^{(l)}$
0	2.667E0	-8.000E0	5.333E0	2.400E1
1	-1.600E1	-5.867E1	3.911E1	1.227E2
2	-4.953E1	-1.788E2	1.192E2	3.905E2
3	-8.573E1	-2.859E2	1.906E2	6.316E2
4	-7.633E1	-2.595E2	1.730E2	5.831E2
5	-4.649E1	-1.569E2	1.046E2	3.540E2
6	-1.956E1	-6.688E1	4.459E1	1.519E2
7	-6.326E0	-2.148E1	1.432E1	4.882E1
8	-1.546E0	-5.319E0	3.546E0	1.215E1
9	-3.133E-1	-1.063E0	7.086E-1	2.421E0
10	-4.923E-2	-1.713E-1	1.142E-1	3.928E-1

Table 2: The coefficients $\boldsymbol{P}^{(l)}$ of the expansion of $\boldsymbol{P}(x, a_s)_{x\to 0}$ in eq. (24) in terms of $a_s(a_s \ln^2 x)^l$ for three and four quark flavours.

The leading small-x off–diagonal elements of $\boldsymbol{P}(x, a_s)_{x\to 0}$ are related by

$$P_{qg,l}^{x\to 0}(x)/(T_F N_f) = -P_{gq,l}^{x\to 0}(x)/C_F \qquad (26)$$

for all l. Also the case of an $\mathcal{N} = 1$ supersymmetric Yang–Mills field theory, i.e. $C_A = C_F = 1$, $N_f = 1$, and $T_F = 1/2$, has been considered. The so–called supersymmetric relation

$$P_{qq,l}(x) + P_{gq,l}(x) - P_{qg,l}(x) - P_{gg,l}(x) = 0 \qquad (27)$$

is satisfied for the small-x leading terms. In fact even more restrictive relations are fulfilled in this case, cf. ref. [18]. Finally it should be noted that there is no overlap of the present small-x resummation with the large-N_f expansion [19] of the all–order splitting function matrix.

3.3. The unpolarized singlet case

Unlike the cases discussed in the previous sections, where the leading small-x singularity in the complex N plane is situated at $N = 0$, the corresponding poles of the anomalous dimensions for the unpolarized singlet evolution are located at $N = 1$. The all–order resummation of the most singular contributions as $x \to 0$, $\gamma_L(N, a_s)$, to the anomalous dimensions was derived in [1]. It is found as the solution of

$$N = 4C_A a_s \chi[\gamma_L(N, a_s)] \,, \qquad (28)$$

with

$$\chi(\gamma) \equiv 2\psi(1) - \psi(\gamma) - \psi(1-\gamma) \,. \qquad (29)$$

Here $\psi(z)$ denotes the logarithmic derivative of Euler's Γ-function. γ_L is a multi-valued function for complex N. The perturbative branch is selected by requiring

$$\gamma_L(N, a_s) \to \frac{4C_A\, a_s}{N-1} \quad \text{for} \quad |N| \to \infty \qquad (30)$$

when solving eq. (28). The singularity structure of the solution in the complex N plane was studied in detail in refs. [20,21]. Finally the resummed small-x contributions $\boldsymbol{\gamma}_L(N)$ to the singlet anomalous dimension matrix $\boldsymbol{\gamma}(N)$, related to the splitting functions in eq. (11) by

$$\boldsymbol{\gamma}(N, a_s) = -2 \int_0^1 dx\, x^{N-1} \boldsymbol{P}(x, a_s) \,, \qquad (31)$$

are in this approximation obtained by

$$\boldsymbol{\gamma}_L(N, a_S) = -2 \begin{pmatrix} 0 & 0 \\ C_F/C_A & 1 \end{pmatrix} \gamma_L(N, a_s) \,. \qquad (32)$$

The $O(a_s)$ correction $\boldsymbol{\gamma}_{\rm NL}(N, a_s)$ to this most singular part as $x \to 0$ have been calculated in ref. [5] for the quark anomalous dimensions $\gamma_{qq,qg}$. In the DIS factorization scheme the matrix of these next-to-leading small-x contributions is given by

$$\boldsymbol{\gamma}_{\rm NL}(N, a_s) = -2 \begin{pmatrix} \frac{C_F}{C_A}[\gamma_{\rm NL} - \frac{8}{3} a_s T_F] & \gamma_{\rm NL} \\ \gamma_{gq,\rm NL} & \gamma_{qg,\rm NL} \end{pmatrix}, \qquad (33)$$

where $\gamma_{\rm NL}$ is used as an abbreviation for the function $\gamma_{\rm NL}^{\rm DIS}(N,a_s)$. It can be recursively expressed by $\gamma_L(N,a_s)$ and reads

$$\gamma_{\rm NL}^{\rm DIS}(N,a_s) = \\ 24T_F a_s \frac{2+3\gamma_L-3\gamma_L^2}{3-2\gamma_L}\frac{[B(1-\gamma_L,1+\gamma_L)]^3}{B(2+2\gamma_L,2-2\gamma_L)}R(\gamma_L) \tag{34}$$

with $B(x,y)$ denoting the Beta function and

$$R(\gamma) = \left[\frac{\Gamma(1-\gamma)\chi(\gamma)}{\Gamma(1+\gamma)\{-\gamma\chi'(\gamma)\}}\right]^{1/2} \\ \exp\left[\gamma\psi(1)+\int_0^\gamma d\zeta\,\frac{\psi'(1)-\psi'(1-\zeta)}{\chi(\zeta)}\right]. \tag{35}$$

The calculation of the yet unknown gluonic entries $\gamma_{gq,\rm NL}$ and $\gamma_{gg,\rm NL}$ in eq. (33) is in progress [22,23]. A first contribution to $\gamma_{gg,\rm NL} \propto N_f$ has been determined recently [23] in the Q_0-scheme [24,25], which has been introduced in the framework of $k_\perp$-factorization.

Both $\boldsymbol{\gamma}_L$ and $\boldsymbol{\gamma}_{\rm NL}$ can be represented by infinite series in a_s. The analytic expressions are straightforwardly obtained but are rather lengthy. The numerical size of the resulting coefficients A_l and B_l in the DIS scheme is illustrated in Table 3. The matrix $\boldsymbol{P}(x,a_s)_{\rm res}$ of the splitting functions including the small–x resummed terms (cf. Section 4.4) beyond the complete LO and NLO matrices from the fixed–order calculations reads:

$$\boldsymbol{P}(x,a_s)_{\rm res}^{\rm DIS} = a_s\boldsymbol{P}_0(x) + a_s^2\boldsymbol{P}_1(x)^{\rm DIS} \\ + \sum_{l=2}^{\infty} A_l\, a_s^{l+1}\frac{1}{x}\ln^l\left(\frac{1}{x}\right)\begin{pmatrix} 0 & 0 \\ C_F/C_A & 1\end{pmatrix} \\ + \sum_{l=1}^{\infty} B_l\, a_s^{l+2}\frac{1}{x}\ln^l\left(\frac{1}{x}\right)\begin{pmatrix} C_F/C_A & 1 \\ 0 & 0\end{pmatrix}. \tag{36}$$

In the subsequent numerical treatment we will use the labels *'Lx'* for results obtained with the leading series (A_l), and *'NLx'* in the cases where the B_l-terms in eq. (36) have been taken into account additionally.

Finally we list the presently available predictions from the small-x resummations for the most singular contributions $P_{ij,2}^{x\to 0}$ of the NNLO splitting functions. There are no $a_s^3\ln^2 x$ terms, due to the matrix structure of eq. (32) and the vanishing of A_2 in eq. (36). For the quark splitting functions [5] the $a_s^3\ln x$ terms read in the DIS scheme

$$P_{qq,2}^{x\to 0}(x)^{\rm DIS} = \left[\frac{568}{9}-\frac{8}{3}\pi^2\right]C_F\,C_A\frac{1}{x}\ln\left(\frac{1}{x}\right). \tag{37}$$

The corresponding $\overline{\rm MS}$ results are given by

$$P_{qq,2}^{x\to 0}(x)^{\overline{\rm MS}} = \frac{224}{9}C_F\,C_A\frac{1}{x}\ln\left(\frac{1}{x}\right), \tag{38}$$

and

$$P_{qg,2}^{x\to 0}(x) = (C_A/C_F)P_{qq,2}^{x\to 0}(x) \tag{39}$$

in both schemes. Unlike the cases discussed in the previous sections, the coefficient functions contain terms as singular as the splitting functions in the $\overline{\rm MS}$ scheme.

l	A_l	B_l
0	1.200E1	$N_f\cdot$ 3.467E1
1	0.000E0	$N_f\cdot$ 4.415E2
2	0.000E0	$N_f\cdot$ 9.528E3
3	8.308E3	$N_f\cdot$ 6.877E4
4	0.000E0	$N_f\cdot$ 4.040E5
5	5.160E4	$N_f\cdot$ 3.411E6
6	8.629E5	$N_f\cdot$ 1.293E7
7	1.721E5	$N_f\cdot$ 5.518E7
8	5.104E6	$N_f\cdot$ 2.601E8
9	2.879E7	$N_f\cdot$ 7.086E8
10	1.433E7	$N_f\cdot$ 2.343E9

Table 3: The coefficients A_l and B_l of the expansion for the small-x resummed splitting functions in the DIS scheme, see eq. (36). For completeness also A_0, A_1 and B_0 are given. For a more precise representation and higher-l terms, cf. refs. [26,27].

3.4. Less singular contributions

The terms in the splitting functions P_{ij} and $P^{\pm}$, which are less singular by one (or more) powers of $\ln(1/x)$ as $x\to 0$ than the leading contributions discussed in the previous sections, are presently unknown in almost all cases. Such subleading contributions, however, can potentially prove to be as important as the leading terms, since the splitting functions and coefficient functions enter observable quantities always via Mellin convolutions with the parton distributions.

This situation can be illustrated by a simple example, cf. ref. [24]. Consider the lowest–order gluonic contribution to the longitudinal structure function $F_L(x,Q^2)$, given by

$$F_L^g(x,Q^2) = 8\,a_s \sum_q e_q^2 \int_x^1 \frac{dy}{y}\, y^2(1-y)\,\frac{x}{y} g(x/y,Q^2)\,. \tag{40}$$

If one replaces the term $1-y$ originating from the coefficient function by its small-y approximation 1 for small values of x, the result for F_L^g changes by a factor of about 4 for typical parametrizations of the gluon density! Due to the Mellin convolution and the fact that $g(x)$ becomes very large as $x \to 0$, the coefficient function at medium and large y contributes essentially. On the other hand the coefficient function in the range $y \gtrsim x$, where the small-y approximation is justified, samples $g(x/y \lesssim 1)$ which is however small. Similar observations can be made for other convolutions considered in the previous sections as well.

The non–singlet '–' and the unpolarized singlet splitting functions are constrained by conservation laws, see eq. (13). The resummed contributions discussed in Sections 3.1 – 3.3 do not obey these constraints, however, less singular terms restore these sum rules. Also for the cases in which the anomalous dimensions are not subject to such constraints, less singular terms with sizeable coefficients exist for example in NLO, e.g. eq. (41).

In order to evaluate the possible impact of such terms, their numerical coefficients have to be estimated. At present the only source of information are the fully known LO and NLO splitting functions. The dominant and subdominant terms as $x \to 0$ for the NLO anomalous dimensions are recalled in eqs. (41)–(43). The results are presented in the general form, as well as, for easier comparison of the numerical size of the coefficients, inserting the number of active flavours as used in the numerical applications in Section 4. In the non–singlet cases one finds in the $\overline{\rm MS}$ scheme

$$\begin{aligned}
\gamma_1^+(N)_{x\to 0} &= -\frac{128}{9N^3} + \frac{400-32N_f}{9N^2} \\
&\overset{N_f=4}{=} -\frac{14.22}{N^3} + \frac{30.22}{N^2}\,,
\end{aligned} \tag{41}$$

$$\begin{aligned}
\gamma_1^-(N)_{x\to 0} &= -\frac{64}{3N^3} + \frac{464-32N_f}{9N^2} \\
&\overset{N_f=4}{=} -\frac{21.33}{N^3} + \frac{37.33}{N^2}\,.
\end{aligned}$$

Note that the subleading terms are roughly of the same size in both cases, despite only one of the combinations being constrained by a sum rule. The corresponding results for the polarized singlet case, also in the $\overline{\rm MS}$ scheme, are given by

$$\begin{aligned}
\gamma_{qq,1}^{\rm pol}(N)_{x\to 0} &= \frac{-64+64N_f}{3N^3} + \frac{464-128N_f}{9N^2} \\
&\overset{N_f=3}{=} +\frac{42.67}{N^3} + \frac{8.889}{N^2}\,, \\
\gamma_{qg,1}^{\rm pol}(N)_{x\to 0} &= +\frac{176N_f}{3N^3} - \frac{24N_f}{N^2} \\
&\overset{N_f=3}{=} +\frac{176.0}{N^3} - \frac{72.00}{N^2}\,, \\
\gamma_{gq,1}^{\rm pol}(N)_{x\to 0} &= -\frac{1408}{9N^3} + \frac{896}{9N^2} \\
&\overset{N_f=3}{=} -\frac{156.4}{N^3} + \frac{99.56}{N^2}\,, \\
\gamma_{gg,1}^{\rm pol}(N)_{x\to 0} &= \frac{-1728+64N_f}{3N^3} + \frac{2088-208N_f}{3N^2} \\
&\overset{N_f=3}{=} -\frac{512.0}{N^3} + \frac{488.0}{N^2}\,.
\end{aligned} \tag{42}$$

The first two terms of the unpolarized singlet anomalous dimensions expanded at $N = 1$ read in the DIS scheme

$$\begin{aligned}
\gamma_{qq,1}^{\rm DIS}(N)_{x\to 0} &= \frac{-832N_f}{27(N-1)} + 2.56 + 100.83N_f \\
&\overset{N_f=4}{=} -\frac{123.3}{N-1} + 405.9\,, \\
\gamma_{qg,1}^{\rm DIS}(N)_{x\to 0} &= \frac{-208N_f}{3(N-1)} + 218.67N_f - 1.78N_f^2 \\
&\overset{N_f=4}{=} -\frac{277.3}{N-1} + 846.2\,, \\
\gamma_{gq,1}^{\rm DIS}(N)_{x\to 0} &= \frac{-864+832N_f}{27(N-1)} - 185.8 - 66.94N_f \\
&\overset{N_f=4}{=} +\frac{91.26}{N-1} - 453.5\,,
\end{aligned} \tag{43}$$

$$\gamma_{gg,1}^{\rm DIS}(N)_{x\to 0} = \frac{184N_f}{3(N-1)} - 629.8 - 93.17N_f + 0.889N_f^2 \stackrel{N_f=4}{=} + \frac{245.3}{N-1} - 988.3\,.$$

One notices that the subleading terms occur in general with signs opposite to those of the dominant ones. Their prefactors are of the same order, but in most cases a factor of about 2 to 4 larger.

Thus introducing subleading terms with prefactors up to two times larger than those of the leading terms appears to yield reasonable and conservative estimates for the possible impact of subleading terms. The following modifications of the resummed anomalous dimensions $\Gamma(N,\alpha_s)$ have accordingly been studied within refs. [13,16,18,20,27]:

$$\begin{array}{ll} \text{A}: & \Gamma(N,\alpha_s) \to \Gamma(N,\alpha_s) - \Gamma(1,\alpha_s) \\ \text{B}: & \Gamma(N,\alpha_s) \to \Gamma(N,\alpha_s)(1-N) \\ \text{C}: & \Gamma(N,\alpha_s) \to \Gamma(N,\alpha_s)(1-2N+N^2) \\ \text{D}: & \Gamma(N,\alpha_s) \to \Gamma(N,\alpha_s)(1-2N+N^3)\ , \end{array} \tag{44}$$

where the replacement $N \to N-1$ is understood for the case of Section 3.3.

Let us finally discuss also the case of the '–' non–singlet evolution in QED. For the evolution kernel also the terms of $O(\alpha^2 \ln x)$ were calculated for e^+e^- annihilation in the on–mass–shell scheme (OMS) in ref. [28]. All contributions but those due to the vacuum polarization diagram cancel in this order. One obtains

$$K_{1,x\to 0}^{-,\rm QED}(x,a)\Big|_{\rm OMS} = -6a^2\left[\ln^2 x + \frac{4}{9}\ln x\right] \leftrightarrow -12\frac{a^2}{N^3}\left[1 - \frac{2}{9}N\right]. \tag{45}$$

Unlike for most of the examples discussed above, in this particular case the term being suppressed by one order in $\ln x$ has thus a smaller coefficient than the leading singular contribution.

4. Numerical consequences

4.1. The unpolarized non-singlet case

The evolution equations (14) for the non–singlet combinations of structure functions can be solved analytically in Mellin-N space. Taking into account the resummed kernels $K_{x\to 0}^{\pm}$ of eq. (16) in addition to the full splitting functions up to NLO, the solution can be written as [13,16]

$$F^{\pm}(N,a_s) = F^{\pm}(N,a_0)\left(\frac{a_s}{a_0}\right)^{\gamma_0(N)/2\beta_0} \times \left\{\exp\left[\frac{1}{2\beta_0}\int_{a_0}^{a_s} da\,\frac{1}{a^2}\Gamma^{\pm}(N,a_s)\right] + \frac{a_s-a_0}{2\beta_0} \cdot \left[\tilde{\gamma}_1^{\pm}(N) - \frac{\beta_1}{\beta_0}\gamma_0(N) + 2\beta_0\hat{c}_{i,1}^{\pm}(N)\right]\right\}, \tag{46}$$

with

$$\gamma_l(N) = -2\int_0^1 dx\, x^{N-1}P_l(x)\,,$$
$$\hat{c}_{i,l}(N) = \int_0^1 dx\, x^{N-1}c_{i,l}(x)\,, \tag{47}$$

and $a_0 = a_s(Q_0^2)$. Here $\tilde{\gamma}_1^{\pm}(N)$ denotes the two–loop anomalous dimension $\gamma_1^{\pm}(N)$ with the leading $1/N^3$ term subtracted. The effect of this term is included to all orders in the exponential factor, which in turn is obtained from eq. (17) by removing the LO contribution included in $\gamma_0(N)$:

$$\Gamma^{\pm}(N,a_s) = \mathbf{\Gamma}_{x\to 0}^{\pm}(N,a_s) - \frac{a_s}{N}\lim_{N\to 0}\left[N\gamma_0(N)\right] = \mathbf{\Gamma}_{x\to 0}^{\pm}(N,a_s) + a_s\frac{4C_F}{N}\,. \tag{48}$$

The NLO evolution of $F^{\pm}(N,a_s)$ can be recovered from eq. (46) by expanding the exponential to first order in a_s and a_0. The inverse Mellin transformation of the final results back to x-space is performed by a numerical integral in the complex N-plane, see e.g. ref. [29].

The remaining quadrature in (46) can be performed analytically for the '+'-case [16], and has to be done numerically for the '–'-combinations involving the parabolic cylinder function $D_p(z = N/\sqrt{2N_c a_s})$. Additional information can be obtained by expanding the resummed kernels $\Gamma^+(N,a_s)$ and $\Gamma^-(N,a_s)$ in a_s, in the latter case using the asymptotic expansion of $D_p(z)$ [12].

The evolution of the '–'-combination

$$xF_3^N(x,Q_0^2) \equiv \frac{1}{2}\left[xF_3^{\nu N}(x,Q_0^2) + xF_3^{\bar{\nu}N}(x,Q_0^2)\right] = c_{F_3}^-(x,Q_0^2) \otimes [xu_v + xd_v](x,Q_0^2) \tag{49}$$

for an isoscalar target N and the '+'-combination

$$F_2^{ep}(x,Q_0^2) - F_2^{en}(x,Q_0^2) = \qquad (50)$$
$$c_{F_2}^{+}(x,Q_0^2) \otimes \frac{1}{3}\big[xu_v - xd_v - 2(x\bar{d} - x\bar{u})\big](x,Q_0^2)$$

have been investigated in refs. [13,16]. As in all other numerical examples displayed below, the reference scale for the evolution (46) is chosen as $Q_0^2 = 4$ GeV^2, and the same input parameters are employed for the NLO and the resummed calculations. In the present case, the initial parton distributions have been adopted from the MRS(A) global fit [30] together with the value of the QCD scale parameter, $\Lambda_{\overline{\rm MS}}(N_f = 4) = 230\,$MeV.

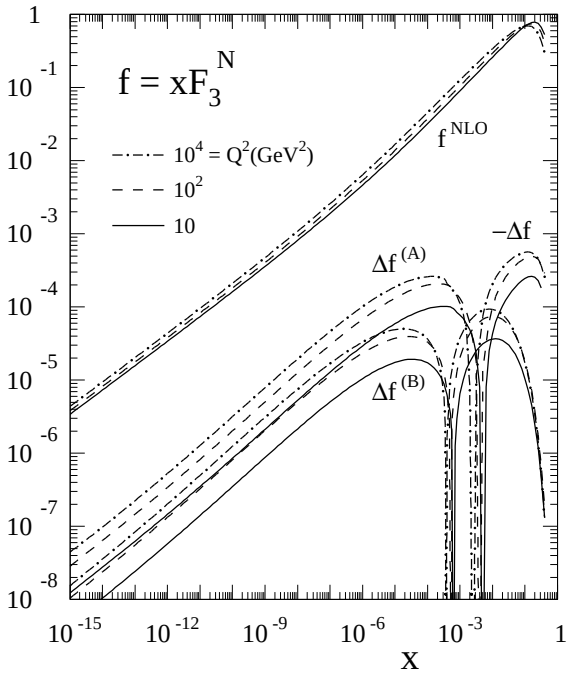

Figure 1: The small-x Q^2-evolution of the non–singlet isoscalar structure function xF_3^N in NLO and the absolute corrections to these results due to the resummed kernels of Section 3.1. '(A)' and '(B)' denote two prescriptions for implementing fermion number conservation, see eq. (44).

The small-x behaviour of the most relevant initial distributions is given by $xu_v(x,Q_0^2) \sim x^{0.54}$ and $xd_v(x,Q_0^2) \sim x^{0.33}$ [30]. Hence these distributions

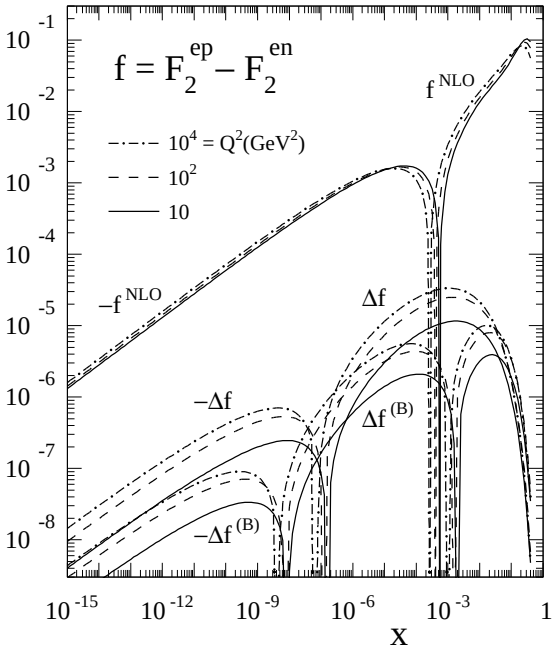

Figure 2: The same as in Figure 1, but for the structure function combination $F_2^{ep} - F_2^{en}$. Instead of the prescription '(A)', the result without any subleading terms is shown for this '+'-case.

are rather 'steep': their rightmost singularities in the complex N-plane lie about 0.5 units or more to the right of the leading singularity of the non–singlet anomalous dimensions at $N = 0$.

In Figures 1 and 2 the NLO results for xF_3^N and $F_2^{ep} - F_2^{en}$ are shown, together with the corresponding resummation corrections, down to x as low as $x = 10^{-15}$. Even at these extremely small values of x, the effect of the resummed anomalous dimensions stays at the level of 1% or below. This is in striking contrast to the expectation of ref. [31], where corrections of up to factors of 10 in the HERA kinematical regime were anticipated. Moreover the resummation effects remain very sensitive to presently unknown terms less singular as $x \to 0$ in the splitting functions. This is illustrated by the impact of the prescription (B) of eq. (44), which removes as much as about two thirds of the resummation effect even at asymptotically low x.

Another interesting issue is the a_s-expansion of the resummed kernel $\mathbf{\Gamma}^{\pm}_{x\to 0}$ (17) mentioned before. In Figure 3 the resummation corrections

with $\Gamma^{\pm}(N, a_s)/a_s$ in eq. (46) expanded to order l are compared to the full results for the cases with no subtraction at one typical value of Q^2.

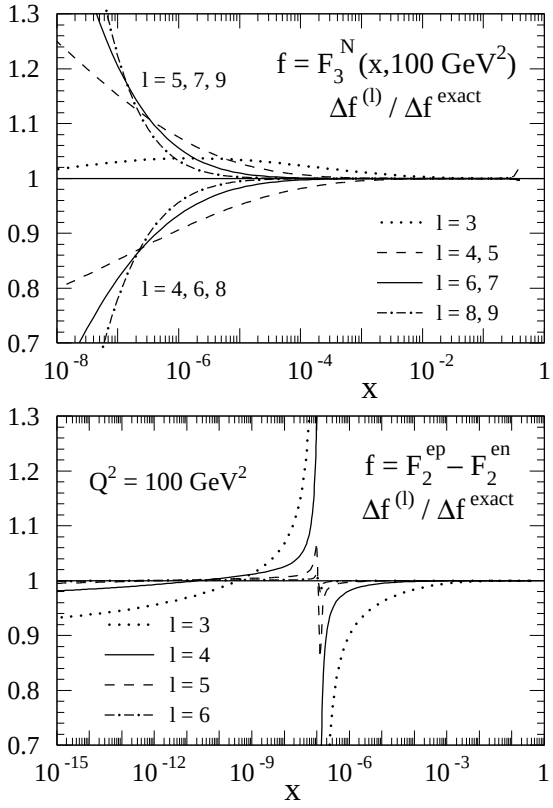

Figure 3: The ratio of the resummation corrections with the resummed anomalous dimensions $\mathbf{\Gamma}^{\pm}_{x\to 0}$ expanded at order a_s^{l+1} to the complete effects for the '–'-quantity F_3^N (upper part) and the '+'-combination $F_2^{ep} - F_2^{en}$ (lower part).

The asymptotic series for the '–'-case leads to a good approximation at $x \gtrsim 10^{-6}$, but starts to diverge below. In the '+'-case, on the other hand, the Taylor series converges in the whole x-range considered. In both cases the next two terms beyond NLO, $l = 3$, contribute more than 90% of the final resummation effect, again even down to $x = 10^{-15}$. The reduced stability for $F_2^{ep} - F_2^{en}$ around $x = 10^{-7}$ is immaterial, since Δf changes sign here.

4.2. The polarized non–singlet case

The solution of the evolution equations proceeds in the same way as in the previous section, see eqs. (46)–(48). The present case is however practically even more interesting. Firstly the non–singlet structure functions are, unlike in the unpolarized case, not a priori suppressed versus their singlet counterparts at very low x. Secondly the shapes of the polarized parton densities are not well established yet [33] by the experimental results. This is illustrated in Figure 4, where the small-x extrapolations of the structure function $g_1^{ep} - g_1^{en}$ (see eq. (51) below) are compared for two choices of the initial distributions.

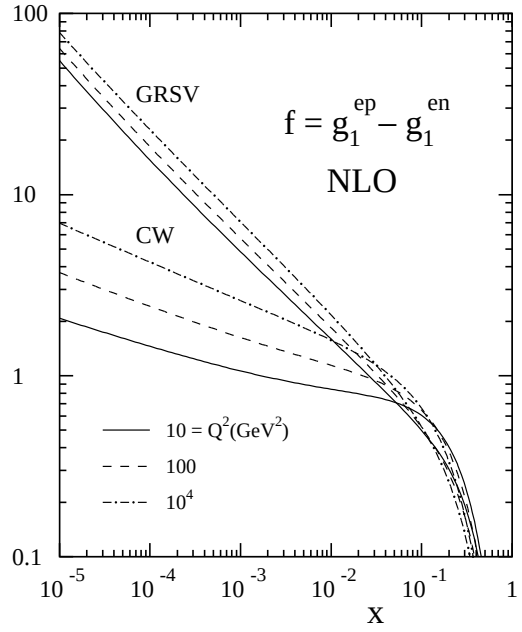

Figure 4: The NLO evolution of the polarized non–singlet structure function combination $g_1^{ep} - g_1^{en}$ for the input densities from refs. [34] and [35].

At small x the valence quark densities of CW [34] are relatively flat: Δu_v, $\Delta d_v(x, 10\,\mathrm{GeV}^2) \sim x^{-0.17,+0.29}$. The more recent distributions of GRSV [35] are on the other hand approximately as steep as the unpolarized distributions, $\Delta u_v(x, Q_0^2) \sim x^{-0.28}$ and $\Delta d_v(x, Q_0^2) \sim x^{-0.67}$. For the evolution of the former (latter) input $\Lambda_{\overline{\rm MS}}(N_f = 4) = 230$ (200) MeV is employed in this section.

The effect of the resummed anomalous dimensions $\mathbf{\Gamma}^{\pm}_{x\to 0}$ (17) has been investigated in refs. [13,16] for the '–'-combination

$$g_1^{ep}(x,Q_0^2) - g_1^{en}(x,Q_0^2) = \qquad (51)$$
$$c^-_{g_1}(x,Q_0^2) \otimes \frac{1}{6}\big[\Delta u_v - \Delta d_v + 2(\Delta\bar{u} - \Delta\bar{d})\big](x,Q_0^2)\,.$$

Here also the '+'-case of the γZ-interference structure function [36] is considered:

$$g^{ep}_{5,\gamma Z}(x,Q_0^2) = c^+_{g_5}(x,Q_0^2) \otimes \frac{1}{4}[\Delta u_v + \Delta d_v](x,Q_0^2)\,. \qquad (52)$$

The resummation corrections for $g_1^{ep} - g_1^{en}$ and $g^{ep}_{5,\gamma Z}$ are shown in Figures 5 and 6, respectively.

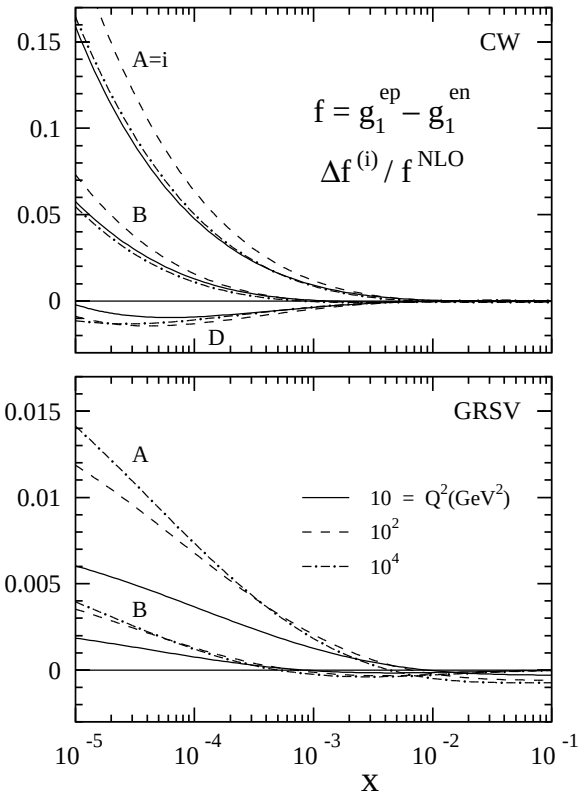

Figure 5: Relative corrections to the NLO small-x Q^2-evolution of the '-'-combination $g_1^{ep} - g_1^{en}$ due to the resummed kernel of Section 3.1 for the initial distributions of refs. [34] and [35]. 'A', 'B', and 'D' denote different prescriptions for implementing fermion number conservation, see eq. (44).

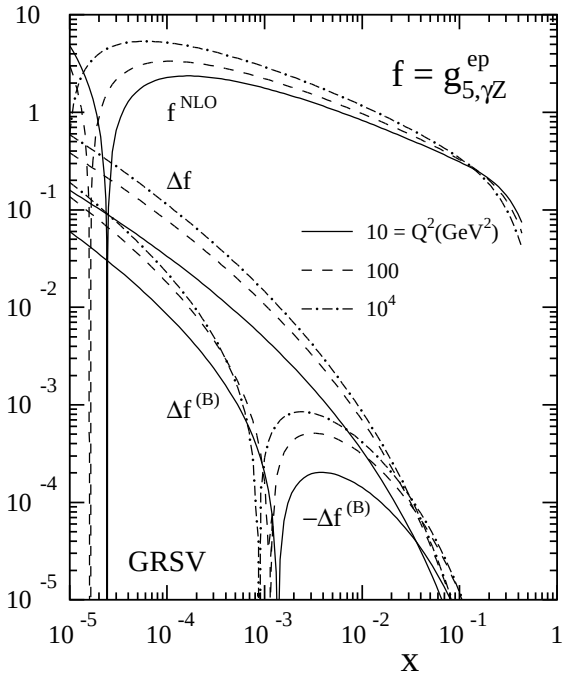

Figure 6: The small-x evolution of the non–singlet interference structure function $g^{ep}_{5,\gamma Z}$ in NLO and the resummation corrections to these results. The possible importance of less singular terms in the higher–order splitting functions is illustrated by the prescription '(B)' for this '+'-case.

For the relatively flat CW input [34], the resummation effect on $g_1^{ep} - g_1^{en}$ reaches 15% at $x = 10^{-5}$. However, in the restricted kinematical range accessible in possible future polarized electron–polarized proton collider experiments at HERA [37], it amounts to only 1% or less. For the steeper GRSV initial distributions [35], the effect is of order 1% or smaller in the whole x range, as in the unpolarized cases considered above. Hence also here the results do not come up to previous expectations of huge corrections up to factors of 10 or larger [32] in the HERA range. The outcome is very similar for $g^{ep}_{5,\gamma Z}$, see Figure 6.

As for the unpolarized non–singlet structure functions, the resummation results also in the polarized cases are not stable against possible subleading contributions in the higher–order anomalous dimensions. With respect to the a_s expansions of the kernels $\mathbf{\Gamma}^{\pm}_{x\to 0}$ (17) the situation is also similar to the unpolarized cases.

4.3. The polarized singlet case

The solution for the singlet part of the evolution equation (8) cannot be given in a closed form beyond leading order. This difference to the non–singlet case is due to the non–commutativity of the splitting functions matrices $\boldsymbol{P}_l(x)$ in eq. (11) for different orders in the strong coupling a_s. Thus the solution has to be written down as a power series in a_s, in N-space resulting in

$$\boldsymbol{q}(N,a_s) \;=\; \Big[1+\sum_{l=1} a_s^l\,\boldsymbol{U}_l(N)\Big]\left(\frac{a_s}{a_0}\right)^{\boldsymbol{\gamma}_0(N)/2\beta_0} \Big[1+\sum_{l=1} a_0^l\,\boldsymbol{U}_l(N)\Big]^{-1}\boldsymbol{q}(N,a_0)\,. \quad (53)$$

Here $\boldsymbol{\gamma}_0(N)$ is related to the matrix of the LO splitting function $\boldsymbol{P}_0(x)$ as in eq. (47), and as before $a_0 = a_s(Q_0^2)$. The singlet evolution matrices $\boldsymbol{U}_l(N)$ can be expressed in terms of the anomalous dimensions $\boldsymbol{\gamma}_{k\le l}(N)$. Technical details can be found in ref. [27].

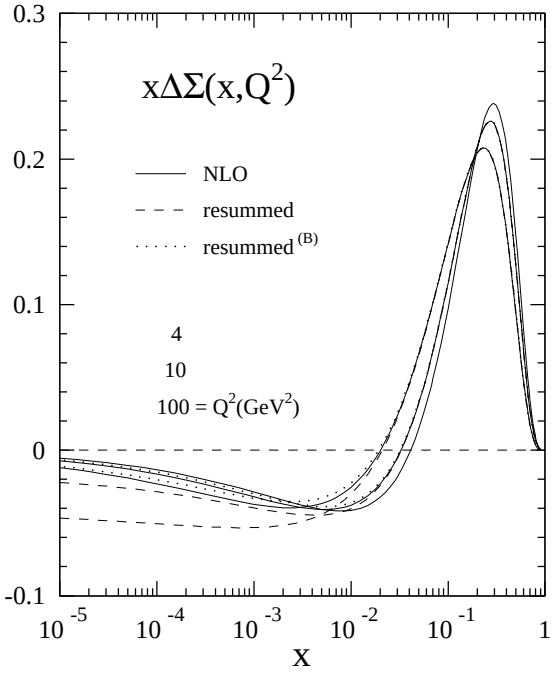

Figure 7: The evolution of the polarized singlet combination $x\Delta\Sigma$ in NLO and including the resummed kernels. The impact of possible subleading terms is illustrated by the prescription '(B)' in eq. (44). The input densities are from ref. [35].

The numerical consequences of the resummation in Section 3.2 on the polarized parton densities and the structure functions g_1^{ep} and g_1^{en} have been investigated in ref. [18]. In Figures 7 and 8 the results are displayed for the polarized singlet and gluon densities, $x\Delta\Sigma$ and $x\Delta g$, respectively. The initial distributions at $Q_0^2 = 4$ GeV^2 have been adopted from the GRSV 'standard' parametrization [35]. The evolution has been performed for $\Lambda_{\overline{\rm MS}}(N_f = 4) = 200\,$MeV, and – different from all other cases shown in this paper – with only three active quark flavours in the splitting functions [35,38], i.e. $\Delta\Sigma$ is given by

$$\Delta\Sigma = \Delta u + \Delta\bar{u} + \Delta d + \Delta\bar{d} + \Delta s + \Delta\bar{s}\,. \quad (54)$$

As in the corresponding non–singlet '–'-case, the expanded solution (53) represents an asymptotic series, which diverges at very small values of x. For all the experimentally relevant cases, $x \gtrsim 10^{-5}$, retaining 8 – 10 terms in eq. (53) is however adequate for obtaining accurate results.

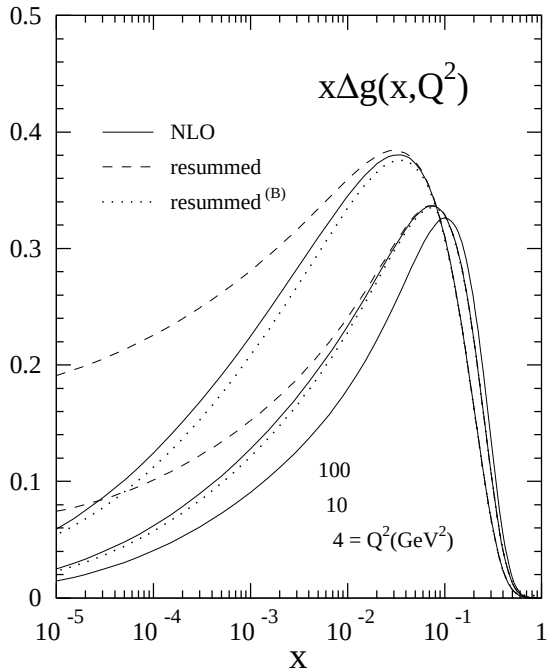

Figure 8: As in Figure 7, but for the polarized gluon momentum distribution $x\Delta g$. As in the previous figure, the Q^2-values in the legend are ordered according to the sequence of the curves at small x.

Figures 7 and 8 show that the resummation effects are much larger for $\Delta\Sigma$ and Δg than for the non–singlet quantities considered in Section 4.2, as to be expected from the comparison of the expansion coefficients in Tables 1 and 2. E.g., the ratio of the (unsubtracted) resummed results to the NLO evolution amounts to about 1.72 (1.64) for $\Delta\Sigma$ (Δg) at $Q^2 = 10$ GeV^2 and $x = 10^{-4}$.

Also illustrated in these figures [by the results for the prescription '(B)' in eq. (44)] is the possible impact of the yet uncalculated terms in the higher–order anomalous dimensions which are down by one power of N with respect to the resummed leading pieces as $N \to 0$. The effect of these additional terms can be very large, in the present example the resummation correction beyond NLO is practically cancelled.

Q^2	10 GeV^2		100 GeV^2	
x	10^{-4}	10^{-3}	10^{-4}	10^{-3}
$x\Delta\Sigma$	-0.0100 -0.0285 -0.0473	-0.0169 -0.0396 -0.0560	-0.0171 -0.0505 -0.0855	-0.0218 -0.0523 -0.0772
$x\Delta g$	0.019 0.101 0.201	0.034 0.152 0.294	0.053 0.226 0.432	0.071 0.281 0.528

Table 3: A comparison of the resummed evolution of the polarized parton distributions for different assumptions on the gluon distribution Δg. Upper lines: minimal gluon, middle lines: standard set, lower lines: maximal gluon (and corresponding quark distributions) of ref. [35] at $Q_0^2 = 4$ GeV^2.

The small-x evolution depends strongly also on the virtually unknown [33] gluon input density. This is obvious from Table 3, where the resummed results of Figures 7 and 8 are compared at two representative values of x and Q^2 to those obtained by evolving in the same way the 'minimal Δg' and 'maximal Δg' distributions of GRSV [35]. The variations are up to a factor of almost 5 (10) for $\Delta\Sigma$ (Δg), respectively. Thus both the unknown less singular terms in the anomalous dimensions and the present bounds on Δg, which are rather weak still, are the dominant sources of uncertainty at small x.

4.4. The unpolarized singlet case

The solution of the evolution equations for the unpolarized singlet parton densities is analogous to the polarized case considered in the previous section, see eq. (53). The present case is special – and has therefore attracted much interest over the past years – since only here precise measurements have been performed for small x, at HERA [40]. The quantitative impact of the resummation discussed in Section 3.3 has been studied for parton distributions and structure functions in refs. [20] and [27]. The latter analysis confirms and extends the former one. Related investigations have been carried out in refs. [26,39].

Below the results are shown for initial distributions which, although representing a somewhat simplified input, incorporate all features relevant to this study in a sufficiently realistic way, especially the small-x powers as supported by HERA structure function data [40]. Specifically, we take in the DIS factorization scheme at $Q_0^2 = 4$ GeV^2:

$$\begin{aligned} xu_v &= A_u x^{0.5}(1-x)^3, \;\; xd_v = A_d x^{0.5}, (1-x)^4 \\ xS &= \Sigma - xu_v - xd_v \quad = A_S x^{-0.2}, (1-x)^7 \\ xg &= A_g x^{-0.2}(1-x)^5, \;\; xc = x\bar{c} = 0\,. \end{aligned} \tag{55}$$

The evolution is performed for four active (massless) flavours, using $\Lambda_{\overline{\rm MS}}(N_f = 4) = 250$ MeV. The (SU(3)–symmetric) sea is assumed to carry 15% of the proton's momentum at the input scale; together with the sum rules this fixes the prefactors A_i.

Figures 9 and 10 compare the resummation results separately for the Lx [1] and NLx [5] series (c.f. Section 3.3) to the standard NLO evolution. In the Lx case, as expected from the matrix structure in eq. (32), the main effect is exerted on the gluon density xg. The impact on the quark evolution is rather moderate. Specifically, the ratio to the NLO results amounts to about 1.3 (1.03) for xg (xS), respectively, at $Q^2 = 10$ GeV^2 and $x = 10^{-4}$, taking the prescription '(A)' of eq. (44) for restoring the energy–momentum sum rule. Including also the NLx quark terms [5], on the other hand, results only in a small further modification of the gluon evolution, whereas the quark distributions are drastically affected. The ratios to the

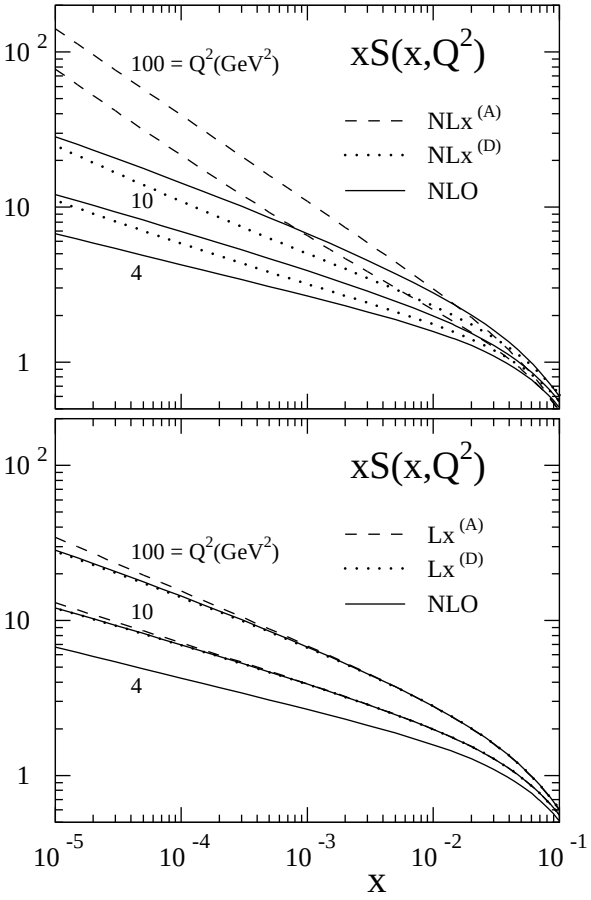

Figure 9: The small-x evolution of the total unpolarized sea quark density xS including the resummed Lx [1] and NLx kernels [5] as compared to the NLO results. Two prescriptions for implementing the energy–momentum sum rule have been applied, c.f. Section 3.4.

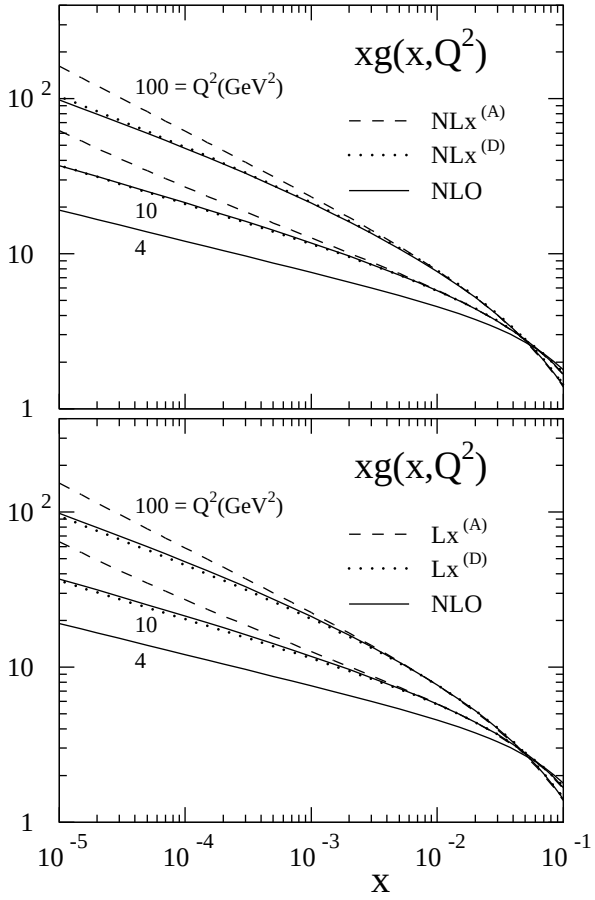

Figure 10: As in Figure 9, but for the unpolarized gluon momentum distribution xg.

NLO results now read 1.3 (3.1) for xg (xS) under the same conditions as before.

A flavour of the possible importance of presently unknown less singular terms in the higher–order anomalous dimensions is provided by the difference of the results of the choices '(A)' and '(D)' in eq. (44). Such terms can be vitally important, like in the polarized case studied in the previous section. As obvious from the figures not even the sign of the deviation from the NLO evolution can be taken for granted.

4.5. QED non–singlet radiative corrections

The resummation of the $O(\alpha \ln^2 x)$ terms may also yield non–negligible contributions to QED radiative corrections [16]. This has been investigated recently for the case of initial–state radiation in deep inelastic eN scattering. In the range of large y the effect can reach around 10% of the differential Born cross section [17], see Figure 11. These terms are not covered by the higher order resummations studied so far [41,42] and reduce their effect [17]. Yet the complete NLO corrections for this process are not known and the size of less singular terms at $O(\alpha^2)$ and their impact on the QED corrections is still to be determined (see, however, eq. (45)).

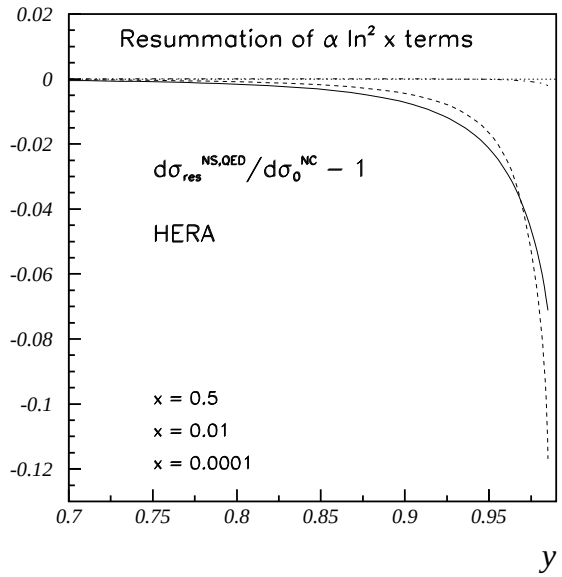

Figure 11: The non–singlet (NS) resummed contribution of the $O(\alpha(\alpha \ln^2 x)^l)$ terms for the QED initial–state correction to the neutral current deep–inelastic scattering cross section at HERA. The results are shown normalized to the differential Born cross section.

For the corresponding corrections to $\sigma(e^+e^- \to \mu^+\mu^-)$ near the Z-peak the situation is different. Since there the QED correction are completely known up to $O(\alpha^2)$ [28], a correction due to the resummation of the $O(\alpha^{l+1} \ln^{2l} x)$ terms is only necessary for the terms beyond two loop order, as in the QCD cases considered before. A numerical study of these effects can also be found in ref. [17].

5. Summary

The resummations of the leading small-x terms in both unpolarized and polarized, non–singlet and singlet anomalous dimensions have been discussed. At NLO the results agree with those found for the most singular terms as $x \to 0$ in fixed–order calculations. The so–called supersymmetric relation is satisfied by the results for the most singular small-x terms to all orders, again for both the unpolarized and polarized cases. These resummations allow the prediction of the leading $x \to 0$ contributions to the 3–loop (NNLO) anomalous dimensions in the $\overline{\rm MS}$ scheme [5,13,16,18]. The coefficient functions are less singular for the non–singlet and polarized singlet cases up to NNLO, $O(\alpha_s^2)$.

For the non–singlet structure functions the corrections due to the $\alpha_s(\alpha_s \ln^2 x)^l$ contributions are about 1% or smaller in the kinematical ranges probed so far and possibly accessible at HERA including polarization [13,16]. The non–singlet QED corrections in deep–inelastic scattering resumming the $O(\alpha \ln^2 x)$ terms can reach values of up to 10% at $x \approx 10^{-4}$ and $y > 0.9$ [17].

In the singlet case very large corrections are obtained for both unpolarized and polarized parton densities and structure functions [18,20,27]. As in the non–singlet cases possible less singular terms in the higher order anomalous dimensions, however, are hardly suppressed against the presently resummed leading terms in the evolution: even a full compensation of the resummation effects cannot be excluded.

To draw firm conclusions on the small-x evolution of singlet structure functions also the next less singular terms have to be calculated. Since contributions even less singular than these ones may still cause relevant corrections, it appears to be indispensable to compare the corresponding results to those of future complete three–loop calculations.

Acknowledgements : We would like to thank W. van Neerven and T. van Ritbergen for useful discussions. This work was supported in part by the EC Network 'Human Capital and Mobility' under contract No. CHRX–CT923–0004, and by the German Federal Ministry for Research and Technology (BMBF) under contract No. 05 7WZ91P (0).

REFERENCES

1. Y. Balitsky and L. Lipatov, Sov. J. Nucl. Phys. **28** (1978) 822.
2. R. Kirschner and L. Lipatov, Nucl. Phys. **B213** (1983) 122.
3. J. Bartels, B. Ermolaev, and M. Ryskin, DESY 96–025.
4. W. Furmanski and R. Petronzio, Z. Phys.

C11 (1982) 293.
5. S. Catani and F. Hautmann, Nucl. Phys. **B427** (1994) 475.
6. S. Larin, T. van Ritbergen, and J. Vermaseren, Nucl. Phys. **B427** (1994) 41;
   S. Larin, P. Nogueira, T. van Ritbergen, and J. Vermaseren, NIKHEF 96–010, `hep-ph/9605317`.
7. D. Gross and F. Wilczek, Phys. Rev. **D8** (1974) 416; **D9** (1974) 980;
   H. Georgi and D. Politzer, Phys. Rev. **D9** (1974) 416;
   L. Lipatov, Sov. J. Nucl. Phys. **20** (1975) 94;
   G. Altarelli and G. Parisi, Nucl. Phys. **B126** (1977) 298;
   K. Kim and K. Schilcher, Phys. Rev. **D17** (1978) 2800;
   Yu. Dokshitser, Sov. Phys. JETP **46** (1977) 641.
8. K. Sasaki, Progr. Theor. Phys. **54** (1975) 1816;
   M. Ahmed and G. Ross, Phys. Lett. **B56** (1975) 385; Nucl. Phys. **B111** (1976) 298;
   G. Altarelli and G. Parisi, ref. [7]
9. G. Floratos, D. Ross, and C. Sachrajda, Nucl. Phys. **B129** (1977) 66, E: **B139** (1978) 545; Nucl. Phys. **B152** (1979) 493;
   A. Gonzalez–Arroyo, C. Lopez, and F. Yndurain, Nucl. Phys. **B153** (1979) 161;
   A. Gonzalez–Arroyo and C. Lopez, Nucl. Phys. **B166** (1980) 429;
   G. Floratos, P. Lacaze, and C. Kounnas, Phys. Lett. **B98** (1981) 89; Nucl. Phys. **B192** (1981) 417;
   G. Curci, W. Furmanski and R. Petronzio, Nucl. Phys. **B175** (1980) 27.
10. G. Floratos, P. Lacaze, and C. Kounnas, Nucl. Phys. **B192** (1981) 417;
    A. Gonzalez-Arroyo and C. Lopez, Nucl. Phys. **B166** (1980) 429;
    G. Floratos, P. Lacaze, and C. Kounnas, Phys. Lett. **B98** (1981) 285;
    W. Furmanski and R. Petronzio, Phys. Lett. **B97** (1980) 437.
11. R. Mertig and W. van Neerven, Z. Phys. **C70** (1996) 637;
    W. Vogelsang, Phys. Rev. **D54** (1996) 2023; RAL–TR–96–020, `hep-ph/9603366`.
12. I. Ryshik and I. Gradstein, Tables of Series, Products, and Integrals, (DVW, Berlin, 1957), 7.340.
13. J. Blümlein and A. Vogt, Phys. Lett. **B370** (1996) 149.
14. For a summary of coefficient functions in the $\overline{\rm MS}$ scheme to $\mathcal{O}(\alpha_s)$ see ref. [4] and references therein.
15. S. Larin and J. Vermaseren, Z. Phys. **C57** (1993) 93;
    E. Zijlstra and W. van Neerven, Nucl. Phys. **B383** (1992) 525; Phys. Lett. **B297** (1993) 377; Nucl. Phys. **B417** (1994) 61; E: **B426** (1994) 245.
16. J. Blümlein and A. Vogt, Acta Phys. Polonica **B27** (1996) 1309.
17. J. Blümlein, S. Riemersma, and A. Vogt, DESY 96–120.
18. J. Blümlein and A. Vogt, DESY 96–050, `hep-ph/9606254`, Phys. Lett. **B**, in print.
19. J. Gracey, LTH–369, `hep-ph/9604426`, these proceedings.
20. K. Ellis, F. Hautmann, and B. Webber, Phys. Lett. **B348** (1995) 582.
21. J. Blümlein, in: Proc. of the XXXth Rencontres de Moriond, *QCD and High Energy Hadronic Interactions*, March 1995, ed. J. Tran Than Van, (Edition Frontieres, Paris, 1996), p. 191; DESY 95–125, `hep-ph/9506446`
22. L. Lipatov, DESY 96–132 and references therein;
    V. del Duca, Phys. Rev. **D54** (1996) 989, EDINBURGH–96–3, `hep-ph/9606427`.
23. G. Camici and M. Ciafaloni, DFF 250/6/96, `hep-ph/9606427`.
24. J. Blümlein, J. Phys. **G19** (1993) 1623.
25. M. Ciafaloni, Phys. Lett. **B356** (1995) 74.
26. R. Ball and S. Forte, Phys. Lett. **B351** (1995) 313.
27. J. Blümlein, S. Riemersma, and A. Vogt, DESY 96–096.
28. F. Berends, G. Burgers, and W. van Neerven, Nucl. Phys. **B297** (1988) 429, E: **B304** (1988) 921.
29. M. Glück, E. Reya, and A. Vogt, Z. Phys. **C48** (1990) 471.
30. A.D. Martin, R. Roberts, J. Stirling, Phys.

Rev. **D50** (1994)
31. B. Ermolaev, S. Manayenkov, and M. Ryskin, Z. Phys. **C69** (1996) 259.
32. J. Bartels, B. Ermolaev, and M. Ryskin, Z. Phys. **C70** (1996) 273.
33. G. Ladinsky, in: Proceedings of the Workshop 'Prospects of Spin Physics at HERA', eds. J. Blümlein and W. Nowak, (DESY, Hamburg, 1995), p. 285 and `hep-ph/9601287`.
34. Hai–Yang Cheng and C. Wai, Phys. Rev. **D46** (1992) 125.
35. M. Glück, E. Reya, M. Stratmann, and W. Vogelsang, Phys. Rev. **D53** (1996) 4775.
36. J. Blümlein and N. Kochelev, Phys. Lett. **B381** (1996) 296.
37. J. Blümlein, DESY 95–164, `hep-ph/9508387`, and Proceedings of the Workshop 'Prospects of Spin Physics at HERA', eds. J. Blümlein and W. Nowak, (DESY, Hamburg, 1995), p. 179.
38. M. Glück, E. Reya, and A. Vogt, Z. Phys. **C67** (1995) 433.
39. J. Forshaw, R. Roberts, and R. Thorne, Phys. Lett. **B356** (1995) 79.
40. For a recent review see, e.g.: F. Eisele, DESY 95–229, invited talk at EPS Conference on High Energy Physics (HEP 95), Brussels, Belgium, 1995. To appear in the proceedings.
41. J. Kripfganz, H. Möhring, and H. Spiesberger, Z. Phys. **C49** (1991) 501.
42. J. Blümlein, Z. Phys. **C65** (1995) 293.